

# Line-based Road Structure Mapping Using Multi-beam LiDAR

Xudong He<sup>1,2</sup>, Junqiao Zhao<sup>\*,1,2</sup>, Lu Sun<sup>1,2</sup>, Yewei Huang<sup>1,2</sup>,  
Xinglian Zhang<sup>1,2</sup>, Jun Li<sup>1,2</sup>, Chen Ye<sup>1,2</sup>

**Abstract**—In this paper, we studied a line-based SLAM method for road structure mapping using multi-beam LiDAR. We propose to use the polyline as the basic mapping element instead of grid cell or point cloud, because the line-based representation is precise and lightweight, and it can directly generate vector-based HD map as demanded by autonomous driving systems. We explored: 1) The extraction and vectorization of road structures based on local probabilistic fusion. 2) The efficient line-based matching between frames of vectorized road structures. A specified road structure, the road boundary, is taken as an example. The results testified the feasibility and effectiveness of the proposed method. We applied our proposed mapping system in three different scenes and achieved the average absolute matching error of 0.07m, the average relative matching error of 8.64%.

## I. INTRODUCTION

The high precision HD map of road environment is now recognized as one of the cornerstones for autonomous driving[1]. The reliable mapping of road boundaries, lanes, and other road structures can greatly abbreviate the workload of on-line perception system, and therefore enhances the performance of autonomous driving in the complex urban environment. However, the conventional method of constructing HD maps still relies on massive manual labor for data post-processing and annotation[2]. Besides, it is even more challenging to update this manually annotated HD map efficiently.

Automatic mapping enabled by SLAM has attracted the attention of many researchers. In visual SLAM, feature-point-based methods have been widely used to build the environment as a map of sparse visual features[3], [4]. Dense methods, on the contrary, directly reconstruct the texture-rich environment into 3D point clouds[5]. Due to the limitations of vision sensors, i.e. the narrow FOV, the short visible range and the dependence of good illumination, LiDARs are preferable since they are able to map the roads and facilities in day and night[2]. The 2D LiDAR-based SLAM is the de facto method for indoor mapping[6], [7]. These methods make use of occupancy grid, thus can probabilistically fuse

the observations and achieve consistent maps. However, grid-based representation is not perfect for mapping of linear road structures, since the discretization is redundant. Another map representation for LiDAR SLAM is based on raw point clouds. Various extensions of ICP matching methods have been investigated for aligning frames of point clouds[8]. [9] has proposed a method for matching between scans using point and line features, thus it can efficiently produce high-quality reconstructions of point cloud. However, the data volume of the point cloud map is even more huge than grid-based map and these methods are usually computationally costly. The detection and mapping of road structures has been explored by [10], [11]. This method can exclude outliers efficiently to get a robust detection of road structures. But the map is optimized based on original point clouds which may lead to poor storage and computational efficiency and, in addition, cannot be vectorized easily.

In conclusion, the current SLAM systems build map either for localization or reconstruction purpose. None of them could directly generate vector-based HD maps as demanded by autonomous driving systems.

In this paper, we propose a line-based method for mapping of road structures. This method is distinguished from previous researches by its polyline-based map representation. This vectorized representation is both lightweight and precise. We explored a combined workflow of road structure detection, vectorization, matching between line-based local maps and optimization. The multi-beam LiDAR sensor is used as the data source thanks to its 360-degree FOV, long observation distance, and high precision. We adopt a specified road structure, the road boundary, in this paper. Others, i.e. the lanes, will be included and discussed in our future work.

The main contributions are:

- The extraction and vectorization of road structures based on the multi-frame probabilistic fusion.
- ICL (Iterative Closed Lines)-based scan-matching method is used to align line-based local maps representing road structures.

## II. RELATED WORK

Road structure map plays a crucial role in navigation and planning tasks of autonomous driving systems, and the performance of road structure mapping relies on robust detection and high-precision matching of road structures. In this part, we will present a brief survey on detection and matching of road structures, respectively.

Both vision sensor and LiDAR are used to detect lane markings and road boundaries. In traditional vision-based

This work is supported by the National Natural Science Foundation of China (No. U1764261), the Natural Science Foundation of Shanghai (No.kz170020173571) and the Fundamental Research Funds for the Central Universities (No. 22120170232)

<sup>1</sup>The Key Laboratory of Embedded System and Service Computing, Ministry of Education, Tongji University, Shanghai zhaojunqiao@tongji.edu.cn

<sup>2</sup>Department of Computer Science and Technology, School of Electronics and Information Engineering, Tongji University, Shanghai

<sup>3</sup>School of Surveying and Geo-Informatics, Tongji University, Shanghai

<sup>4</sup>School of Automotive Studies, Tongji University, Shanghai

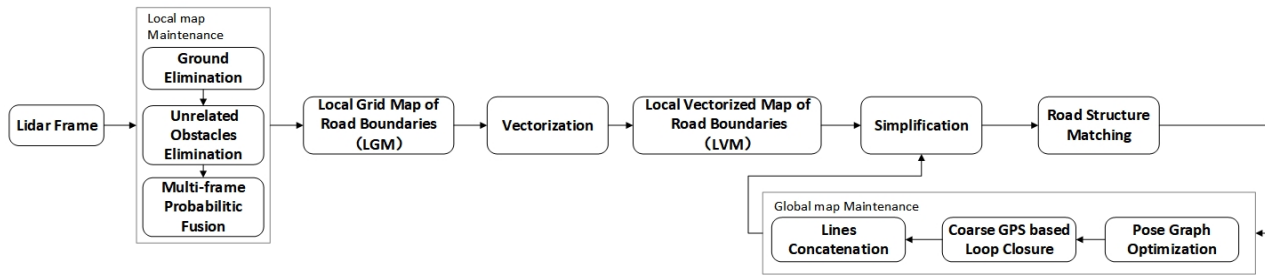


Fig. 1. Overview of the framework.

methods, lane markings can be detected based on scan line or edge detection[12]. Recently, more robust DNN-based segmentation methods were proposed for extracting lanes or even road boundaries [13], [14]. However, the performance of these methods is still vulnerable to various lighting conditions and the narrow FOV of vision sensors. Multi-beam LiDAR can overcome the above shortcomings because of the 360-degree active sensing and high precision measurement. Furthermore, road structures, i.e. boundaries, can be easily interpreted from point clouds rather than from image textures. In [10], curb points candidates was obtained by analyzing the distance between consecutive rings, and filters were then applied to remove false positives. In [15], the road marking detector used an adapted Otsu thresholding algorithm to optimize the segmentation of point clouds based on the intensity, which resulted in asphalt and road markings. However, these methods suffer from the sparsity of point clouds far from the sensor. Therefore, multi-frame fusion is demanded.

The matching between frames is the basis of odometry and SLAM methods. [16] proposed a lane-marking-based matching method using vision data between on-line images and the lane marking map. However, this method was for localization purpose and the lane marking map was built in offline using DGPS and requiring manually refinement. For LiDAR-based methods, scan matching is often applied to match two consecutive point clouds[17], [18], or two 2D/3D grid-based local maps[19], [20], [21]. Little has been explored for directly matching between road structures. Chamfer matching was originally proposed in [22] for finding an object in a cluttered image based on a given line-drawing. Later, this method was extended to trajectory matching[23]. However, this method is suitable for matching between images thus requires textual features, which is scarce in linear road structures. Similar to ICP, ICL adopted extracted 3D linear features to register point clouds using line-to-line distance[24]. PL-ICP adopted point-to-line distance to match between points and a polyline[8]. This method takes into account the geometric features of the polyline, which provide richer structural information, therefore is incorporated in our proposed method.

Without loss of generality, we detect and match one specific road structure, the road boundary, in the following sections.

### III. THE APPROACH

In this chapter, all essential components of the automatic road boundary detection and mapping are presented. This comprises road boundary segmentation, road boundary vectorization, line-based matching and concatenation, and back-end optimization. The pipeline is shown in Fig. 1.

#### A. Road Boundary Segmentation

Segmentation of road boundary from LiDAR scans has been studied and implemented intensively. However, the automatic segmentation from one scan or from multiple simply aligned scans can be problematic because of following reasons: Firstly, the resolution of point clouds decreases exponentially regarding the distance to the sensor. The resulting sparsity has an adverse effect on segmentation of both curbs and lane markings in the far area. Secondly, the simple registration of point clouds from multiple scans based on odometry or even high-precision GPS outputs is subject to minor errors of LiDAR calibration and influences of dynamic objects.

To overcome these problems, we adopt a probabilistic fusion method based on 2D occupancy grid. Multiple scans are firstly fused in the local grid map.

1) *Road Boundary Segmentation*: We use a grid map for representing LiDAR scans. The height related information is needed in ground elimination, and the multi-frame fusion is performed by using occupancy probability, so the information maintained in each grid cell is: maximum height, minimum height, height difference, occupancy probability. At the same time, each grid cell can be extended to store a set of associated 3D points to enable the retrieval of the raw data.

In the first step, the ground is eliminated by obstacle segmentation, which is conducted in two steps: Firstly, the average of  $m$  lowest  $z$  values of points in an upsampled grid cell is counted as  $z_{min}$ . All the points in the upsampled grid cell that are higher than  $z_{min}$  by a certain amount are classified as obstacle points. In the next step, we traverse each of the original grid cells. The cell which contains obstacle points located within the vertical span of the vehicle is marked as an obstacle. After this two steps, all ground area is removed while the grid cells representing obstacles such as road boundaries remained.

In the second step, virtual scans described in Sec. III-B.1 is applied as a preprocessing before fusion. This preprocessing

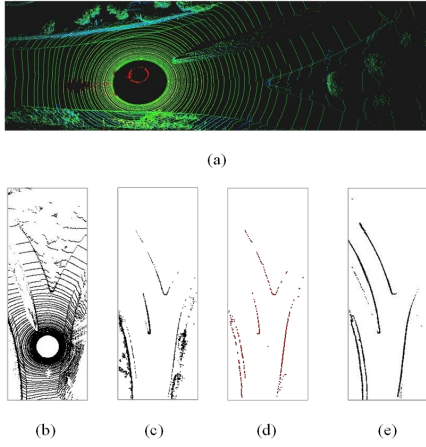


Fig. 2. Road boundary segmentation and probabilistic fusion. (a) 3D point cloud of a scene. (b) 2D projection. (c) Ground elimination. (d) Road boundaries segmented in one frame. (e) Multi-frame probabilistic fusion.

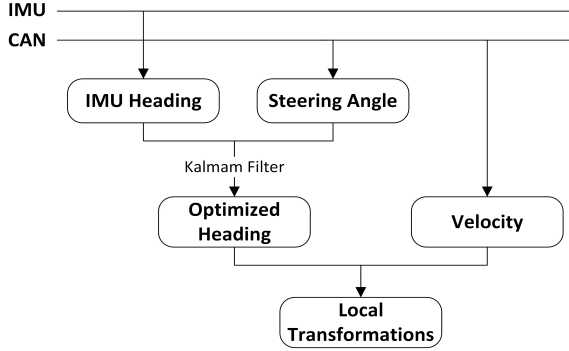


Fig. 3. Kalman filter based odometry

eliminates obstacles unrelated to the road boundary in order to improve the computational efficiency of multi-frame fusion. After the above two steps, we obtain a grid map of road boundaries which need to be enriched by multi-frame fusion (Fig. 2(d)).

2) *Kalman-Filter-based Odometry*: To locally fuse multi-frames with high precision, a simple but accurate reckoning system is developed. We use a combination of two reckoning sources based on heading + velocity and steering + velocity respectively. The heading is read from the IMU’s digital compass and the steering angle and velocity are read from the CAN. We firstly employ a Kalman filter to fuse steering angle and heading. As a result, possible drifting of headings and accumulative errors of steering can be corrected. Afterwards, we integrate the optimized heading and the velocity to calculate transformations of car’s pos in the NED coordinate frame (Fig. 3).

3) *Multi-frame Probabilistic Fusion*: Based on the locally satisfied odometry results, we fuse multiple frames of coarse segmentation. This is based on standard odds updating using occupancy probability maintained in each grid. The previous segmentation results can be greatly enhanced which generate the local grid map (LGM) of road boundaries (Fig. 2(e)).

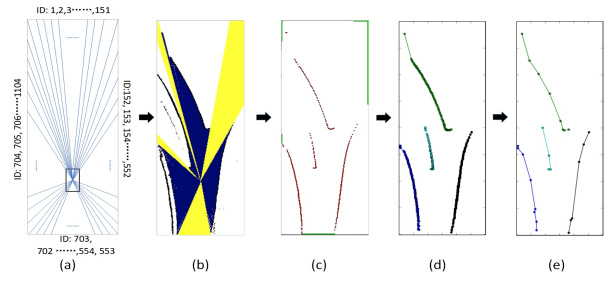


Fig. 4. Road boundary vectorization and simplification. (a) Initially generated virtual scans. (b) Road boundary candidates calculation. (c) Road boundaries candidates clustering (red denotes road boundaries and green denotes free spaces). (d) Road boundaries vectorization. (e) Road boundaries simplification.

## B. Road Boundary Vectorization

1) *Polyline Extraction based on Virtual Scans*: In this section, we propose a vectorization method, which utilizes the virtual scan to vectorize the road boundaries into poly-lines in the LGM. Firstly, a number of virtual scans are initially generated, and the ID of each ray increases in the clockwise order as proposed in [25] (Fig. 4(a)). Then, the points of intersection between each ray and either the grid cell representing road boundary (*hit*) or the border of the grid map (*miss*) are calculated and are considered as road boundary candidates (Fig. 4(b)). According to the ID and the type of the intersection point, i.e. whether *hit* at road boundaries or *miss* at borders of the grid map (shown in Fig. 4(c) by red and green respectively), we can cluster the road boundary candidates into road boundaries and grid boundaries. Moreover, within each cluster, these ordered points can be connected into a vectorized polyline (Fig. 4(d)), and we obtain a local vectorization map (LVM) of road boundaries.

2) *Feature-preserved Simplification*: Since the vectorized result can be noisy and dense due to the selected angular resolution of the virtual scan, we employ the Ramer-Douglas-Peucker algorithm[26] to optimize polylines in the LVM. The simplified representation can be reduced to merely 6% of the points in the original polyline (Fig. 4(e)), which is both lightweight and beneficial to the later matching process. For a clear description in following sections, we term the simplified version of LVM as simplified LVM and the original version as raw LVM.

## C. Line-based Matching and Concatenation

In this paper, a road boundary matching method based on vectorized line features is proposed, which perform efficiently and, more importantly, can concatenate polylines to form an HD map of road boundaries.

1) *Line-based Matching*: To match directly between vectorized road boundaries, a polyline-to-polyline matching method should be proposed. We choose the iterative optimization framework such as ICP for its simplicity and high accuracy. Consequently, the distance metric between polyline and polyline should be formulated. The exact measurement

of distances between polylines or between nodes in a polyline and another polyline can be computationally costly. As a result, a fast approximation by finding the nearest node-to-line correspondence as adopted in PL-ICP[8] is employed. Nevertheless, the polyline generated from the previous step is simplified and nodes are sparse, based on which the correspondence cannot be accurately established. Therefore, we introduce the process of interpolation to generate temporary points between nodes of the polyline, which samples the line segment in a fixed interval. The resulting temporary points are only used to find the node-line correspondence, and will not be fully involved in matching calculations. KD-tree is built to further accelerate the process. The above interpolation is only conducted on the referencing polyline, thus is efficient. Based on the correspondence between polylines, the optimization function is as:

$$G(R, T) = \min \sum_{i=1}^T \|n_{j_1-j_2}^T \cdot [(u_i * R + T) - v_{j_1}]\|^2$$

where  $R$  and  $T$  are rotation and translation between the unregistered polyline and the reference polyline,  $n_{j_1-j_2}$  is the normal of line segment represented by the node pair  $[v_{j_1}, v_{j_2}]$  in the reference polyline after interpolation, the nodes  $u_i$  and  $v_{j_1}$  are the correspondent pair between the two polylines, in which  $u_i$  is the node from the unregistered polyline.

In Sec. IV-C, we will show the simplified-LVM-based matching of road boundary converges faster than raw-LVM-based matching. Besides, vectorizing the road boundary as polylines takes into account the geometric characteristics of the road boundary, thus can improve the precision of matching.

2) *Concatenation*: After matching and optimization, transformed polylines of two frames will overlap. To build the HD map, polylines that representing continuous road boundaries should be concatenated into one unified vectorization.

When performing concatenating, we directly find all the intersection points between two overlapped polylines. We then connect all the intersection points to smoothly merge two polylines into one. The order is preserved by tracing along nodes within each polylines. As a result, line segments are concatenated to get a complete and ordered polyline.

#### D. Back-end Optimization

We adopt  $g^2o$  [27] in our method to construct a pose-graph for optimization. The data association is realized with the help of coarse GPS localization and line-based scan matching described in Sec. III-C. Once a pair of line-based maps is associated, an edge between two poses is added to the graph. The least square problem can then be solved by minimization of the following object function:

$$F(x) = \sum_{k \in frames} e(p_i, p_j, z_{ij})^T \Omega_k e(p_i, p_j, z_{ij})$$

where  $p_i$  and  $p_j$  are associated poses,  $e(p_i, p_j, z_{ij})$  is the residue between two poses  $p_i$  and  $p_j$ ,  $z_k$  and  $\Omega_k$  are the mean and information matrix of the edge.

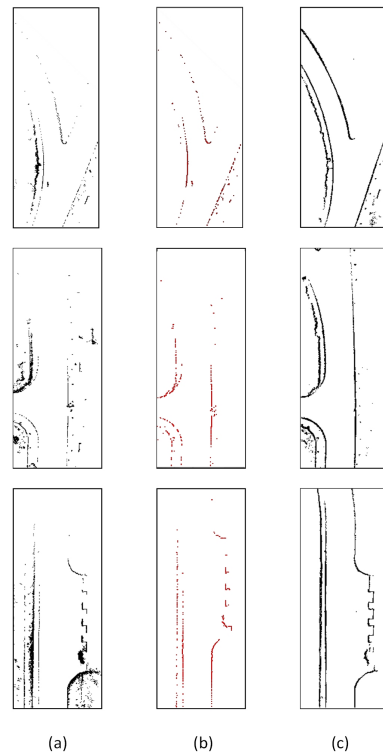


Fig. 5. Road boundary segmentation in three scenes. (a) Ground elimination. (b) Road boundaries segmented in one frame. (c) Local grid map of boundaries (LGM).

Notwithstanding this optimization can be applied straightforwardly, we do not include the results because it is still under implementation and is beyond the contributions proposed in this paper.

## IV. EXPERIMENTAL RESULT

The experiments in this paper are based on the TiEV autonomous driving platform<sup>1</sup>. TiEV is equipped with sensors including Velodyne HDL-64, IBEO lux8, SICK lms511, vision sensors, and the RTK+IMU. In this paper, only the Velodyne HDL-64 is used for perception.

All the experimental datasets are captured at Jiading campus of Tongji University.

#### A. Road boundary Segmentation and Probabilistic Fusion

The 3D point cloud is mapped to a grid map with a map size of 401 by 151 and a resolution of 0.2m. We select 400 frames forward and 100 frames backward for probabilistic fusion to build LGM. Fig. 5(c) shows the results of LGM, comparing with Fig. 5(b), which shows the results of road boundary segmentation in one frame, multi-frame fusion greatly improves the robustness and accuracy of road boundary detection.

#### B. Vectorization and Simplification

Fig. 6(a) shows the extraction of road boundary candidates by using virtual scans, where different colors represent

<sup>1</sup>cs1.tongji.edu.cn/tiev

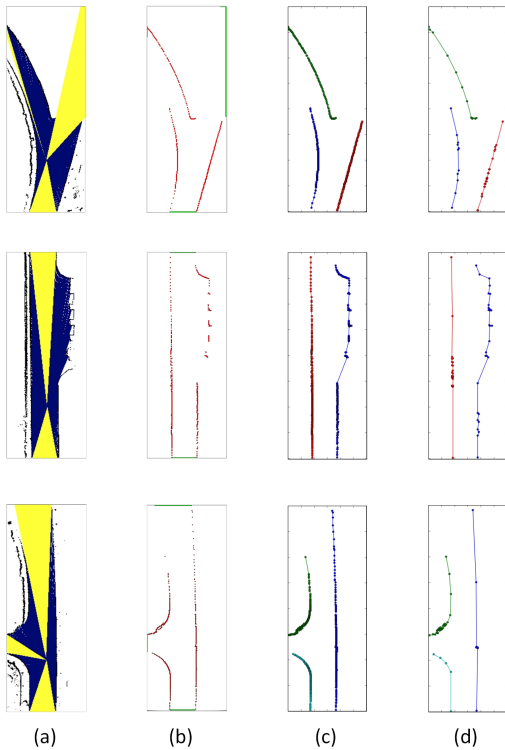


Fig. 6. Vectorization and simplification of road boundaries in three different scenes. (a) Road boundary candidates calculation. (b) Road boundaries clusters (red denotes road boundaries and green denotes free spaces). (c) The raw LVM. (d) The simplified LVM.

different types of road boundary candidates, i.e. *hit* or *miss*. The results of clustering are shown in Fig. 6(b). The initial vectorizations, i.e. the raw LVMs, are generated as shown in Fig. 6(c). Fig. 6(d) shows the simplified LVMs, which are accurate as well as storage and computing efficient.

### C. Line-based Matching and Concatenation

Fig. 7 shows the results of matching of nine LVMs in three different scenes. The results of ICP (based on projected point clouds) and our method (line-based matching of LVMs) are shown for comparison.

In Fig. 7(b), there are many misalignments in the matching results of ICP, which are indicated by the blurred point clouds. Both the matching of the raw LVMs and the matching of the simplified LVMs, are superior to those from ICP, shown by Fig. 7(c) and Fig. 7(d) respectively. The latter obtains the best visual results, and the matched polylines are all concatenated.

In order to qualitatively evaluate the accuracy of matching, we also analyzed the eight matching results of each scene and compared with ground truths from RTK-GPS. As shown in Fig. 8, in different scenes, the accuracy of simplified-LVM-based matching is better than raw-LVM-based matching and ICP matching. In Tab. I, it can be seen that the average absolute errors of simplified-LVM-based matching are less than 0.08m, and the average relative errors are less than 10%, which are superior to the other two matching methods.

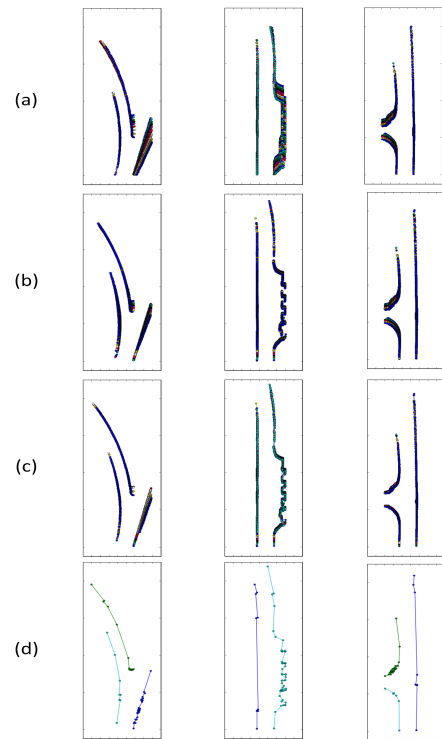


Fig. 7. Road boundary matching in three different scenes. (a) Original unmatched road boundaries. (b) Matched road boundaries using ICP. (c) Matched road boundaries using raw-LVM-based matching. (d) Matched road boundaries using simplified-LVM-based matching and concatenation.

Among them, the relative error is not low because of the short distance between LVMs in the experiment. Tab. II shows that the simplified-LVM-based matching is also more time efficient than the other two matching methods.

In addition, in Fig. 8 and Tab. I, the error in scene B is lower than the other two scenes. This is probably because that there are more structural features presenting. This shows that the proposed matching method is more appropriate to match scenes with rich structural features.

## V. CONCLUSION AND FUTURE WORK

This paper presents a line-based mapping method for road structures, especially the road boundaries. This method could directly generate the vectorized map which is desired by autonomous driving and related applications. We propose to detect road boundaries based on local probabilistic fusion of multi-beam LiDAR scans. The virtual scan and line simplification are employed to vectorize road boundaries into polyline-based representation. During matching, a fast approximation is adopted to achieve the centimeter accuracy between polylines directly. Concatenation of matched polylines finally generate continues and consistent vector map of road boundaries.

Future works include the mapping of a whole area incorporating the lanes, the more efficient concatenation strategy for map updating and the improvement of matching in structural-less road environments.

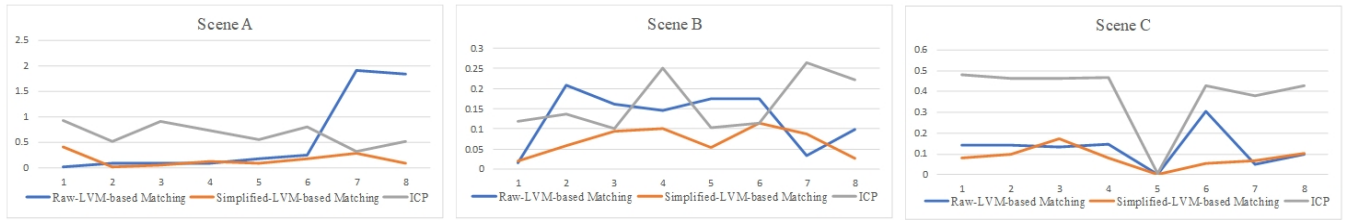


Fig. 8. Eight matching errors between nine LVMS in different scenes

TABLE I  
QUANTITATIVE ERRORS

| Scenes  | Average Absolute Error of Matching (m) |               |                       | Average Relative Error of Matching (%) |               |                       |
|---------|--|---------------|-----------------------|--|---------------|-----------------------|
|         | ICP                                    | Raw-LVM-based | Simplified-LVM-based* | ICP                                    | Raw-LVM-based | Simplified-LVM-based* |
| Scene A | 0.65                                   | 0.55          | 0.07                  | 54.12                                  | 32.33         | 9.48                  |
| Scene B | 0.16                                   | 0.13          | 0.06                  | 17.27                                  | 13.49         | 7.12                  |
| Scene C | 0.38                                   | 0.12          | 0.08                  | 85.91                                  | 24.45         | 9.32                  |

TABLE II  
TIME COST

| Scenes  | Time Cost(ms) |               |                       |
|---------|---------------|---------------|-----------------------|
|         | ICP           | Raw-LVM-based | Simplified-LVM-based* |
| Scene A | 98.05         | 85.39         | 3.98                  |
| Scene B | 58.37         | 43.65         | 3.74                  |
| Scene C | 22.63         | 19.61         | 2.18                  |

## REFERENCES

- [1] H. G. Seif and X. Hu, "Autonomous driving in the icityhd maps as a key challenge of the automotive industry," *Engineering*, vol. 2, no. 2, pp. 159 – 162, 2016. [Online]. Available: <http://www.sciencedirect.com/science/article/pii/S2095809916309432>
- [2] M. Aeberhard, S. Rauch, M. Bahram, and G. Tanzmeister, "Experience, results and lessons learned from automated driving on germany's highways," *IEEE Intelligent Transportation Systems Magazine*, vol. 7, no. 1, pp. 42–57, 2015.
- [3] R. Mur-Artal, J. M. M. Montiel, and J. D. Tardis, "Orb-slam: A versatile and accurate monocular slam system," *IEEE Transactions on Robotics*, vol. 31, no. 5, pp. 1147–1163, 2017.
- [4] G. Klein and D. Murray, "Parallel tracking and mapping for small ar workspaces," in *Mixed and Augmented Reality, 2007. ISMAR 2007. 6th IEEE and ACM International Symposium on*. IEEE, 2007, pp. 225–234.
- [5] J. Engel, T. Schöps, and D. Cremers, "Lsd-slam: Large-scale direct monocular slam," in *European Conference on Computer Vision*. Springer, 2014, pp. 834–849.
- [6] W. Hess, D. Kohler, H. Rapp, and D. Andor, "Real-time loop closure in 2d lidar slam," in *IEEE International Conference on Robotics and Automation*, 2016, pp. 1271–1278.
- [7] J. M. Santos, D. Portugal, and P. R. Rui, "An evaluation of 2d slam techniques available in robot operating system," in *IEEE International Symposium on Safety, Security, and Rescue Robotics*, 2014, pp. 1–6.
- [8] A. Censi, "An icp variant using a point-to-line metric," in *IEEE International Conference on Robotics and Automation*, 2008, pp. 19–25.
- [9] J. Zhang and S. Singh, "Loam: Lidar odometry and mapping in real-time," in *Robotics: Science and Systems*, vol. 2, 2014.
- [10] A. Y. Hata, F. S. Osorio, and D. F. Wolf, "Robust curb detection and vehicle localization in urban environments," in *Intelligent Vehicles Symposium Proceedings*, 2014, pp. 1257–1262.
- [11] A. Y. Hata and D. F. Wolf, "Feature detection for vehicle localization in urban environments using a multilayer lidar," *IEEE Transactions on Intelligent Transportation Systems*, vol. 17, no. 2, pp. 420–429, 2016.
- [12] A. Borkar, M. Hayes, and M. T. Smith, "A novel lane detection system with efficient ground truth generation," *IEEE Transactions on Intelligent Transportation Systems*, vol. 13, no. 1, pp. 365–374, 2012.
- [13] B. Huval, T. Wang, S. Tandon, J. Kiske, W. Song, J. Pazhayampallil, M. Andriluka, P. Rajpurkar, T. Migimatsu, and R. Cheng-Yue, "An empirical evaluation of deep learning on highway driving," *Computer Science*, 2015.
- [14] V. Badrinarayanan, A. Kendall, and R. Cipolla, "Segnet: A deep convolutional encoder-decoder architecture for image segmentation," *arXiv preprint arXiv:1511.00561*, 2015.
- [15] A. Hata and D. Wolf, "Road marking detection using lidar reflective intensity data and its application to vehicle localization," in *IEEE International Conference on Intelligent Transportation Systems*, 2014, pp. 584–589.
- [16] M. Schreiber, C. Knoppel, and U. Franke, "Laneloc: Lane marking based localization using highly accurate maps," in *Intelligent Vehicles Symposium*, 2013, pp. 449–454.
- [17] E. B. Olson, "Real-time correlative scan matching," in *IEEE International Conference on Robotics and Automation*, 2009, pp. 1233–1239.
- [18] S. Rusinkiewicz and M. Levoy, "Efficient variants of the icp algorithm," in *International Conference on 3-D Digital Imaging and Modeling, 2001. Proceedings*, 2002, pp. 145–152.
- [19] D. Hahnel, W. Burgard, D. Fox, and S. Thrun, "A highly efficient fast-slam algorithm for generating cyclic maps of large-scale environments from raw laser range measurements," in *Proceedings of the IEEE/RSJ International Conference on Intelligent Robots and Systems, IROS*, 2003.
- [20] P. Biber and W. Straßer, "The normal distributions transform: A new approach to laser scan matching," in *Intelligent Robots and Systems, 2003. (IROS 2003). Proceedings. 2003 IEEE/RSJ International Conference on*, vol. 3. IEEE, 2003, pp. 2743–2748.
- [21] S. Agarwal, K. Mierle, and Others, "Ceres solver," <http://ceres-solver.org>.
- [22] H. G. Barrow, J. M. Tenenbaum, R. C. Bolles, and H. C. Wolf, "Parametric correspondence and chamfer matching: Two new techniques for image matching," *Proc.int.joint Conf.artificial Intelligence*, vol. 2, no. 11, p. 1961, 1977.
- [23] G. Floros, B. V. D. Zander, and B. Leibe, "Openstreetslam: Global vehicle localization using openstreetmaps," in *IEEE International Conference on Robotics and Automation*, 2013, pp. 1054–1059.
- [24] M. Alshawa, "lcl: Iterative closest line a novel point cloud registration algorithm based on linear features," *Ekscentar*, vol. 10, no. 10, pp. 53–59, 2007.
- [25] M. Montemerlo, J. Becker, S. Bhat, H. Dahlkamp, D. Dolgov, S. Ettinger, D. Haehnel, T. Hilden, G. Hoffmann, and B. Huhnke, "Junior: The stanford entry in the urban challenge," *Journal of Field Robotics*, vol. 25, no. 9, pp. 569–597, 2008.
- [26] D. K. Prasad, M. K. Leung, C. Quek, and S.-Y. Cho, "A novel framework for making dominant point detection methods non-parametric," *Image and Vision Computing*, vol. 30, no. 11, pp. 843–859, 2012.
- [27] R. Kummerle, G. Grisetti, H. Strasdat, K. Konolige, and W. Burgard, "G2o: A general framework for graph optimization," in *IEEE International Conference on Robotics and Automation*, 2011, pp. 3607–3613.